

## Dynamic simulation of the system pantograph-catenary-vehicle-track

A. Ramos<sup>2</sup>, J.R. Jimenez-Octavio<sup>1</sup>, M. Such<sup>3</sup>, A. Carnicero<sup>1</sup>, C. Sánchez<sup>1</sup>.

*1Institute for Research in Technology. ETSI-ICAI, Universidad Pontificia Comillas, Alberto Aguilera, 23, 28015 Madrid, Spain. carnicero@dim.icaei.upcomillas.es.; 2ENUSA, Madrid, Spain; 3European Space Agency, ESTEC, TEC-MSS. Noordwijk, The Netherlands*

### Abstract

This paper presents an advanced pantograph-catenary-vehicle-track model which allows the coupled simulation of the complete system. The model developed is able to evaluate the contact force generated in the catenary-pantograph and wheel-track interactions. Nevertheless, this paper focuses on the possible influence of the vehicle-track system in the catenary-pantograph dynamic interaction. Moreover, the effects of considering track irregularities and short-bridge ways are analyzed. The techniques employed in the simulation are widely known and therefore the formulation of its equations is not studied in depth.

### 1. Introduction

In railway systems, the catenary-pantograph interaction is the phenomenon responsible of the transmission and the raising of the electric energy from the power supply to the locomotive. The quality of this raising, the circulation speed and the maintainability of the infrastructure depend on the design and the running of this system. There are many analyses of the dynamic behavior of the system, so it is worthy to mention the surveys related to this topic realized in [1,2], the simulation of the catenary-pantograph dynamics using a finite element method (FEM in the following) presented in [3], the simplified models which are developed in [4] and improved in [5] or the mathematical model of [6].

As far as the drive system of the most of trains is based on the wheel-track contact, the study of the global dynamic of this system is known as vehicle-track interaction. Obviously, the quality of this contact affects on the passenger comfort, the noise emission and the maintainability of the set amongst others. There exist many studies about the global dynamic of the vehicle-track set: using moving loads and moving elements in both works [7] and [8] respectively; while an analysis of this interaction and its influence on the traffic when trains pass over bridges is presented in [9] and [10].

### 2. Catenary- Pantograph mode

The catenary model employed in this work is based on a FEM discretization of the catenary geometry (Figure 1). In order to reach an accurate performance of the cable system: the contact and messenger wires that have been employed are based on a co-rotational beam formulation; while the droppers have been modeled with truss elements which present also a co-rotational formulation. Moreover, these elements are not capable to resist compression efforts, so the possible slackening of the droppers is taken into account. The catenary used in the simulations presented in this paper is the Re-250, which is employed in the Madrid-Sevilla high speed service.

## Challenge E: Bringing the territories closer together at higher speeds

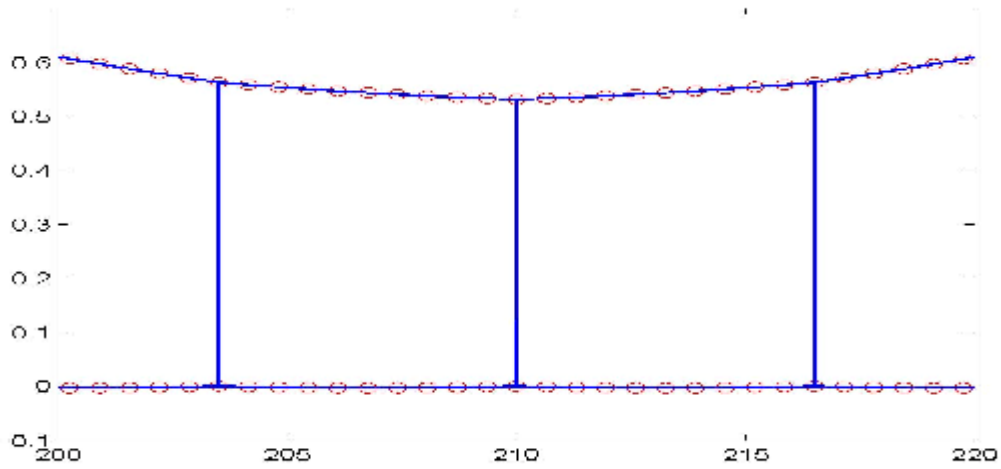


Figure 1. FEM mesh of a span of the catenary model

The pantograph model, on the contrary, has been carried out with a lumped-mass system, as it is usual in this kind of simulations, since its precision is generally enough. In addition, the pantograph has been preloaded with a constant force of  $157.3\text{ N}$ .

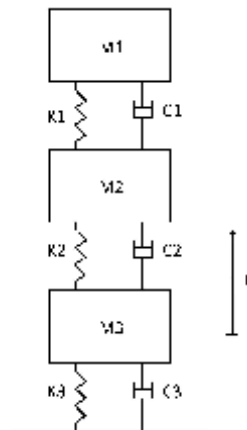


Figure 2. Pantograph model

The three-degrees-of-freedom pantograph depicted in Figure 2 has been simulated with the mass, damp and stiffness values collected in Table 1, which belong to the DSA-380E pantograph. Finally, the contact between the pantograph and the contact wire has been modeled using a penalty method, due to the simplicity of its implementation.

	1	2	3
M (kg)	6.6	5.8	5.8
C(Ns/m)	70	70	70
K(N/m)	$9.4 \cdot 10^3$	$14.1 \cdot 10^3$	0.08

Table 1: Simulation values of DSA-380E pantograph

### 2.1 Catenary-Pantograph interaction model

The dynamic performance of the catenary-pantograph system has been validated in accordance with the European standard EN50318 [11]. This standard establishes the requirements for the validation of a catenary-pantograph interaction computational model. Essentially, this norm establishes a benchmark theoretical catenary-pantograph system and the range of results that must be accurately predicted by a simulation code. Table 2 shows a comparison of the obtained values over the referenced model previously described and the required by the aforementioned standard.

Speed (km/h)	250		300	
	Validation Range	Model	Validation Range	Model
Mean contact force (N)	110 – 120	116.07	110 – 120	115.35
Standard Deviation (N)	26 – 31	27.38	32 – 40	33.64
Max. Statistic value (N)	190 – 210	198.20	210 – 230	216.27
Min. Statistic value (N)	20 – 40	33.91	-5 – 20	14.44
Max. Real value (N)	175 – 210	177.57	190 – 225	210.35
Min. Real value (N)	50 – 70	60.05	30 – 55	40.87
Max. uplift at support 1 (mm)		53.4		62.7
Max. uplift at support 2 (mm)	48 – 55	51.9	55 – 65	63.1
Max. uplift at support 3 (mm)		53.0		62.0
Percentage of the loss of contact	0 %	0 %	0 %	0 %

Table 2: Validation of the catenary-pantograph model

### 3. Vehicle model

The vehicle model has been carried out with a ten-degrees-of-freedom lumped-mass system linked by truss bars as is shown in the diagram shown in Figure 3. This sort of models behaves more accurately than the simpler ones of three-degrees-of-freedom without an excessive added computational cost. Moreover, its modular nature allows fitting the lower part of the pantograph and the upper part of the vehicle by means of imposing that both displacements are equal.

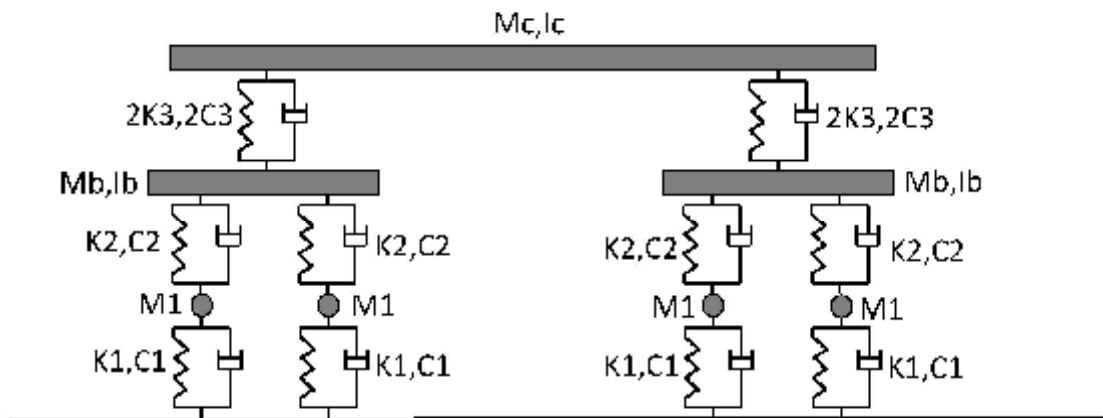


Figure 3.10 DOF vehicle model

Their stiffness and inertia values have been taken equivalent to the vehicles simulated. Thus in the simulations carried out, the values collected in Table 3, which belong to the 103 series of AVE train taken from [13,14], have been used.

### Challenge E: Bringing the territories closer together at higher speeds

	1	2	3
$M$ (kg)	350	0	0
$C$ (Ns/m)	$6.7 \cdot 10^5$	0	0.4
$K$ (N/m)	$8 \cdot 10^9$	$0.3 \cdot 10^6$	$4.4 \cdot 10^6$
$m_b$ (kg)	$5.84 \cdot 10^4$		
$I_b$ (m <sup>4</sup> )	$1 \cdot 10^{-3}$		
$m_c$ (kg)	$6.19 \cdot 10^4$		
$I_c$ (m <sup>4</sup> )	$1 \cdot 10^{-3}$		

Table 3: Numeric values of the 103 serie of AVE

#### 4. Track model

The track model has been realized by a beam over an elastic foundation as seen in Figure 4. Its stiffness gathers the most important features of the track. This makes it possible to simulate changes of the subsoil conditions, through varying the stiffness of the springs, or the addition of surface defects on the rails by modifying the geometric position of the beams.

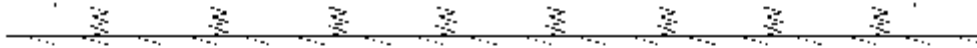


Figure 4. Track model

Real values of the Madrid-Barcelona high speed service, see Table 4, have been considered in the simulations that are presented in this paper.

Track	Value
$E$ (GPa)	210
$I$ (cm <sup>4</sup> )	3313
$A$ (cm <sup>2</sup> )	28
$\rho$ (kg/m <sup>3</sup> )	7800
Platform	
$K$ (MN/m)	15.79
Distance between sleepers (m)	0.6

Table 4. Properties of the rail and platform considered

The study about french tracks carried out by Fryba, presented in [12], shows that irregularities of a track can be considered as a random variable whose power spectral density function depends on the quality of the track. So, the different types of tracks are split up from the lowest (1) to the highest (6) quality class which characterizes this random variable. It is also possible to include variations on the theoretical position of the track by the generation of a spatial series whose power spectral density is:

$$PSD_{ir}(\omega_j) = \frac{A\omega_2^2(\omega_j^2 + \omega_1^2)}{\omega_j^4(\omega_j^2 + \omega_2^2)}$$

where the parameters  $A$ ,  $\omega_1$ ,  $\omega_2$  depend on the quality of the track, see Table 5. Thus, once the theoretical random positions are generated it is possible to consider the position of the track from a more realistic point of view.

Class	1	2	3	4	5	6
$A$ (mm)	15.53	8.85	4.92	2.75	1.57	0.98
$\omega_1$	23.3					
$\omega_2$	13.1					

Table 5: Values for the random irregularities simulation

Figure 5 shows the power spectral density function and two series of irregularities compatible with the spectrum for two different class of track.

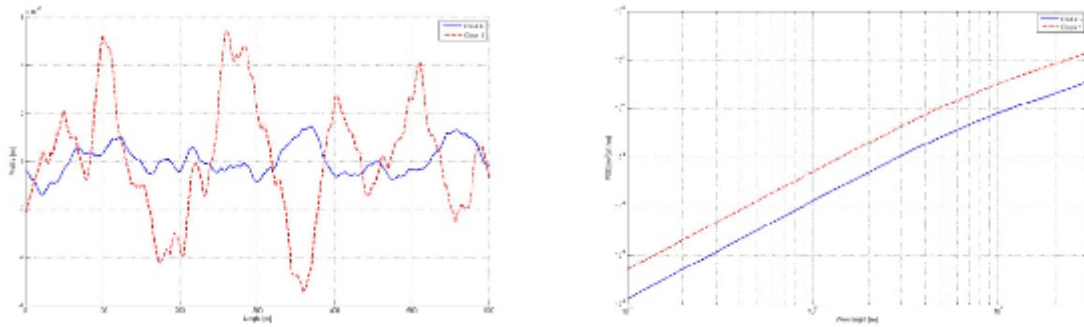


Figure 5. Random profiles and PSD functions

Likewise, it is possible to simulate the traffic of the vehicle over viaducts, which are modeled as the beam depicted in Figure 6 in case of having short viaducts or by using a more complex FEM model in case of having longer viaducts.

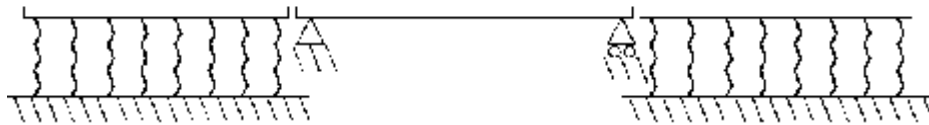


Figure 6. Track and short bridge model

The short viaducts presented in this paper have been simulated with the properties referred in [13], which are reproduced in the following Table 6.

Length (m)	E (GPa)	A (m <sup>2</sup> )	I (m <sup>4</sup> )	$\rho$ (kg/m <sup>3</sup> )
5	29.43	0.8974	0.0154	7800
7.5	29.43	1.1538	0.0565	7800
10	29.43	1.2821	0.0881	7800
20	29.43	2.5641	1.7214	7800

Table 6: Characteristic values for short viaducts

#### 4.1 Vehicle-Track interaction model

The set vehicle-track model has been validated by means of a reference simulation and the comparison of the obtained results against the values gathered in [8]. Figure 7 reflects this comparison: the displacements of the track that have been calculated using the model presented in this paper and the values obtained from the previously mentioned one.

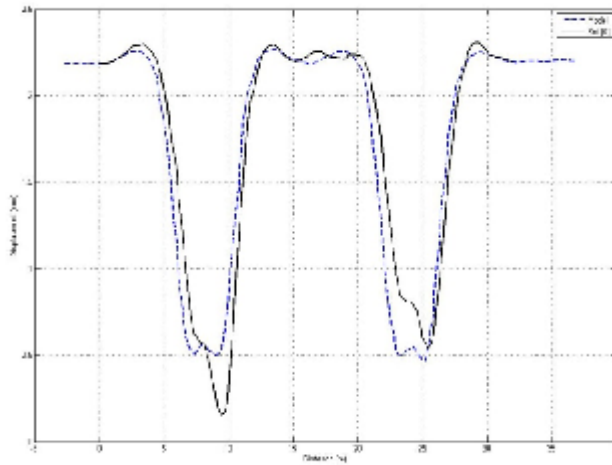


Figure 7. Validation of the vehicle-track model

### 5. Simulations and results

Both simulations of the catenary-pantograph set (CP), without considering the vehicle-track set, and simulations that take into account this set and the existence of random irregularities and the traffic over short viaducts have been realized. So, for the last one a coupled model catenary-pantograph-vehicle-track (CPVT) has been carried out as it is represented in Figure 8.

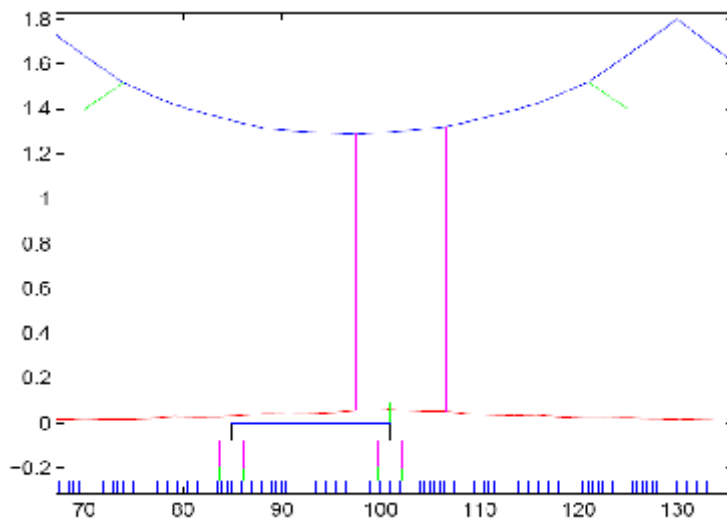


Figure 8. Coupled model CPVT

The basic isolated simulation of the catenary-pantograph dynamic interaction establishes the reference point of this study. Afterwards, these simulation values will be useful to analyze the effect of the vehicle-track model over the catenary-pantograph dynamics. This dynamic interaction has been performed applying a time integration scheme  $\alpha$ -generalized, obtaining the following results of Table 7:

Speed(km/h)	200	250	300	325
MinimumContactForce(N)	69.55	57.33	45.04	29.03
MaximumContactForce(N)	165.78	208.89	218.7	227.91
MeanContactForce(N)	120.14	119.93	119.63	118.55
Standard deviationContact Force (N)	18.98	25.37	30.342	35.74
Range pantograph displacement (mm)	31.4	26.4	28.3	30.6

Table 7: Values of the catenary pantograph simulation

#### 5.1 Track Irregularities

### Challenge E: Bringing the territories closer together at higher speeds

The results of the coupled simulation CPVT using a track with random irregularities of quality class 6 are shown in Table 8. This table presents the values of contact force and contact point displacement history for each traffic speed. Moreover, the percentage difference with the reference point of Table 7 is also tabulated for each case.

Speed (km/h)	200		250		300		325	
Mean C.F. (N)	120.56	0.35%	119.6	-0.28%	119.99	0.30%	118.86	0.26%
Maximum C.F. (N)	169.9	2.42%	211.64	1.30%	219.15	0.21%	227.79	-0.05%
Minimum C. F.(N)	70.78	1.74%	53.14	-7.88%	45.33	0.64%	29.51	1.63%
Standard Desv. C.F. (N)	19.41	2.22%	25.69	1.25%	30.25	-0.3%	36.05	0.86%
Range panto. Disp (mm)	29.00	8.28%	28.82	8.40%	30.34	6.72%	32.97	7.19%

Table 8: Values of the simulation CPVT with random irregularities

The influence of the track profile in the response of the vehicle can be seen in Figure 9, where the response of the top of the vehicle is showed in a track without irregularities together with two different random profiles of irregularities of quality class 1. The presence of these irregularities increases the displacements of the vehicle.

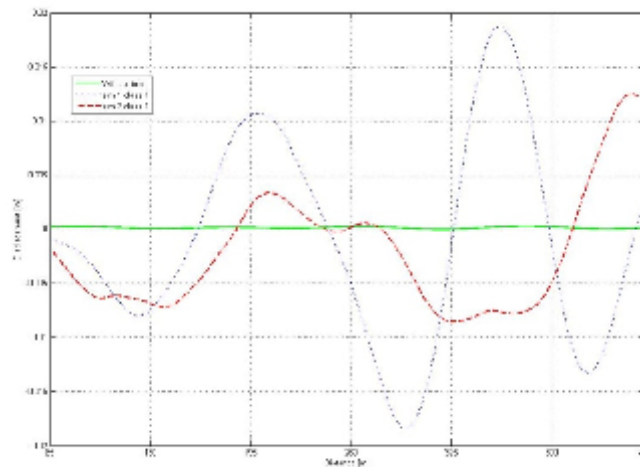


Figure 9. Vehicle response for different track profiles

The following figure, divided into two subfigures, illustrates a pantograph displacement comparison. In the left side of Figure 10 is depicted the vertical displacement of the contact point, which is almost the same considering the system catenary-pantograph with and without the system vehicle-track (note that the red line overlaps the blue one). The right side of this figure shows the differences in the pantograph displacements among different kind of track quality classes. The displacement conserves its basic tendency although little differences in amplitude can be observed.

## Challenge E: Bringing the territories closer together at higher speeds

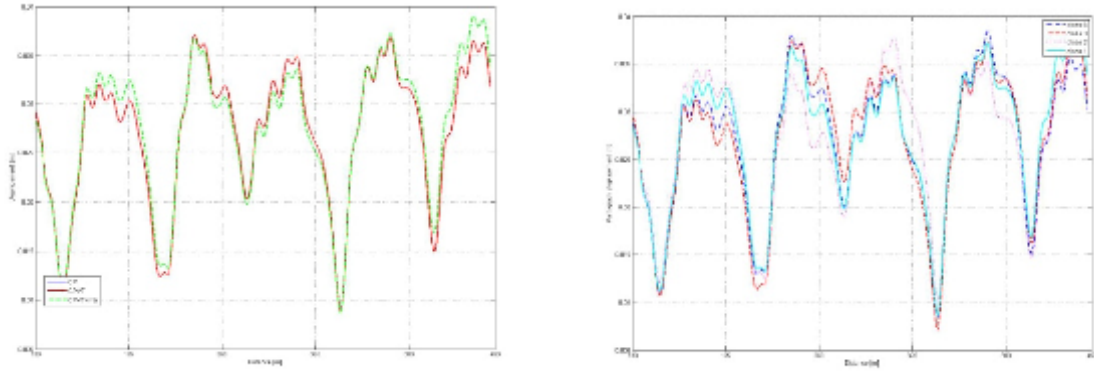


Figure 10. Pantograph displacement comparison

Figure 10 and particularly Figure 11 also show that the frequency content of the signal is not modified for the presence of the system vehicle-track. Thus, Figure 11 presents the spectrum of the pantograph displacement.

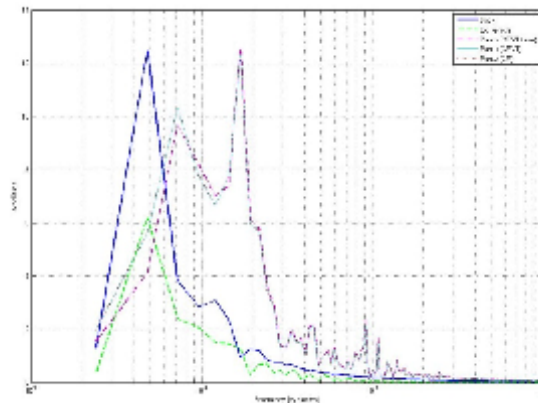


Figure 11. Pantograph displacement spectrum

### 5.2 Short Bridges

The simulations that have been performed considering the traffic over short bridges have been compared with the results of the contact force in the case of just simulating the set CP. The percentage differences are contained in Table 9.

Length (m)	5	7.5	10	20	Speed(km/h)
Minimum	-0.31	-1.14	-2.88	-5.47	200
Maximum	0.35	0.96	2.8	3.98	
Standard Desv	0.11	0.23	0.56	1.13	
Range	0.66	2.1	5.78	9.45	
Minimum	-0.6	-0.75	-1.92	-3.44	250
Maximum	0.98	1.30	2.55	3.3	
Standard Desv	0.36	0.45	0.92	1.47	
Range	1.58	2.06	4.47	6.74	
Minimum	-1.82	-1.15	-2.04	3.14	300
Maximum	1.11	1.23	1.97	3.22	
Standard Desv	0.41	0.32	0.53	0.98	
Range	2.92	2.37	4.01	6.36	
Minimum	-0.71	-1.01	-0.64	-2.86	325
Maximum	0.74	0.75	1.26	3.28	
Standard Desv	0.16	0.16	0.78	1.01	
Range	1.45	1.75	1.91	6.14	

Table 9: Differences [%] in the traffic over short bridges



## 6. Conclusions

In view of the results presented on the previous sections, it is possible to conclude that the vehicle-track system introduces differences lower than 3% in the contact force of the catenary-pantograph interaction due to track irregularities. Thus, although these differences can be neglected, the displacements in the pantograph reach differences between 6% and 8% in the worst quality class of the track. However, these differences would be decreased in case of considering higher quality of the track. In case of considering the traffic over short viaducts the differences can be up to 10%.

## 7. Acknowledgements

This work has been partially funded by the Spanish Ministerio de Ciencia e Innovación under the project "Simulation of the wind effect in the interaction of catenary-pantographs of high speed trains" (TRAN2009-13912-C\_02-02/TREN). This support is gratefully acknowledged.

## 8. References

- [1] G.Poetsch, J.Evans, R.Meisinger, W.Kortüm, W.Baldauf, A.Veitl and J.Wallaschek, Pantograph/catenary dynamics and control, *Vehicle System Dynamics*, (1997) 28: 159–195.
- [2] A.A.Shabana and J.R.Sany, A survey of rail vehicle track simulations and flexible multibody dynamics, *Nonlinear Dynamics*, (2001) 26: 179–210.
- [3] A.Collina and S.Bruni, Numerical simulation of pantograph-overhead equipment interaction, *Vehicle System Dynamics*, (2002) 38 (4): 261–291.
- [4] T.X.Wu and M.J.Brennan, Dynamic stiffness of a railway overhead wire system and its effect on pantograph-catenary system dynamics. *Journal of Sound and Vibration*, (1999) 219 (3):483-502.
- [5] O.Lopez-Garcia, A.Carnicero and J.L.Maroño, Influence of stiffness and contact modelling on catenary pantograph system dynamics, *Journal of Sound and Vibration*, (2007) 299:806-821.
- [6] M.Arnold and B.Simeon, Pantograph and catenary dynamics: a benchmark problem and its numerical solution, *Applied Numerical Mathematics*, (2000) 34 (4): 345–362.
- [7] M.Olsson, Finite element, modal co-ordinate analysis of structures subjected to moving loads, *Journal of Sound and Vibration*, (1985) 99:1-12.
- [8] C.G.Koh, J.S.Y.Ong, D.K.H.Chua and J.Feng, Moving element method for train-track dynamics, *International Journal for Numerical Methods in Engineering*, (2003) 56:1549–1567.
- [9] Ping Lou and Qing-yuan Zeng, Formulation of equations of motion of finite element form for vehicle-track-bridge interaction system with two types of vehicle model, *International Journal for Numerical Methods in Engineering*, (2005) 62:435-474.
- [10] Ping Lou, Vertical dynamic responses of a simply supported bridge subjected to a moving train with two-wheelset vehicles using modal analysis method, *International Journal for Numerical Methods in Engineering* (2005) 64:1207-1235.
- [11] EN50318:2002, Railway applications. Current collection systems. Validation of simulation of the dynamic interaction between pantograph and overhead contact line, European Standard, (2002).
- [12] L. Frýba. Dynamics of railway bridges. Thomas Telford, (1996).
- [13] F.Gabaldón, F.Riquelme, J.M.Goicolea and J.J.Arribas, Dynamic analysis of structures under high speed train loads: case studies in Spain. Dynamics of high-speed railway bridges; Advanced Course, Porto, 20-23 September (2005). Faculty of Engineering, University of Porto.
- [14] M.Melis, Dinámica vertical de la vía, Cátedra de Ferrocarriles ETSICCyP, (2008).

Esta table no esta en el articulo, la creamos solo para la presentacion

Speed (km/h)	200		250		300		325	
Maximum (N)	212.6	1.51%	257.6	4.67%	246.9	1.03%	268.9	5.39%
Minimum (N)	98.41	-1.08%	71.31	-23.2%	69.45	-1.22%	48.66	15.22%
Standard Desv. (N)	22.97	2.83%	31.36	-22.5%	31.61	0.69%	39.7	4.15%
Range (N)	114.14	3.64%	186.29	21.54%	177.45	1.99%	220.24	2.91%

Table 10: Values of the simulation CPVT over large bridges